


Mycobacterium tuberculosis protease MarP activates a peptidoglycan hydrolase during acid stress

Helene Botella¹, Julien Vaubourgeix¹, Myung Hee Lee², Naomi Song¹, Weizhen Xu¹, Hideki Makinoshima^{3,†}, Michael S Glickman³ & Sabine Ehrh^{1,*} 

Abstract

Mycobacterium tuberculosis (Mtb) can persist in the human host in a latent state for decades, in part because it has the ability to withstand numerous stresses imposed by host immunity. Prior studies have established the essentiality of the periplasmic protease MarP for Mtb to survive in acidified phagosomes and establish and maintain infection in mice. However, the proteolytic substrates of MarP that mediate these phenotypes were unknown. Here, we used biochemical methods coupled with supravital chemical probes that facilitate imaging of nascent peptidoglycan to demonstrate that during acid stress MarP cleaves the peptidoglycan hydrolase RipA, a process required for RipA's activation. Failure of RipA processing in MarP-deficient cells leads to cell elongation and chain formation, a hallmark of progeny cell separation arrest. Our results suggest that sustaining peptidoglycan hydrolysis, a process required for cell elongation, separation of progeny cells, and cell wall homeostasis in growing cells, may also be essential for Mtb's survival in acidic conditions.

Keywords acid resistance; mycobacteria; peptidoglycan; protease

Subject Categories Microbiology, Virology & Host Pathogen Interaction; Post-translational Modifications, Proteolysis & Proteomics

DOI 10.15252/embj.201695028 | Received 15 June 2016 | Revised 28 November 2016 | Accepted 2 December 2016 | Published online 5 January 2017

The EMBO Journal (2017) 36: 536–548

Introduction

The alarming rise of antibiotic resistance has challenged the efficacy of antimicrobial therapies and underscored the need for new therapeutics. This need is particularly acute for tuberculosis (TB), the leading bacterial cause of death worldwide in 2014 (<http://www.who.int/tb/en>).

The etiologic agent of TB, *Mycobacterium tuberculosis* (Mtb), is a facultative intracellular pathogen that enters the human host through the airways and initially colonizes the lungs. In pulmonary alveoli, macrophages and dendritic cells phagocytize invading microbes and sequester them in a phagosome, a specialized cellular compartment where they are usually eliminated. During its maturation, the phagosome acquires bactericidal properties and intraphagosomal microbes are exposed to reactive oxygen and nitrogen species, antimicrobial peptides, acidic pH, and nutrient deprivation (Flannagan *et al*, 2009; Weiss & Schaible, 2015). Mtb can stall the maturation of the phagosome until macrophages have been activated by the T-cell-derived cytokine IFN- γ , enhancing acidification of the phagosomal milieu, a stress with which Mtb must cope to survive (Schaible *et al*, 1998; Via *et al*, 1998; MacMicking *et al*, 2003). Moreover, Mtb and *M. marinum* have been found in acidic phagolysosomes early during infection of mice and zebrafish larvae (Levitte *et al*, 2016).

To withstand acidic environments, Mtb requires the serine protease MarP (*Mycobacterium* acid resistance protease). Mtb that lacks MarP (Δ marP) is hypersensitive to acidic pH and fails to maintain its intracellular neutral pH when subjected to pH 4.5 (Vandal *et al*, 2008). The MarP-deficient mutant is attenuated in immunocompetent mice. It did not replicate to the same extent as wild-type (WT) Mtb and failed to persist during chronic infection (Vandal *et al*, 2008). Similarly, *M. marinum* lacking the homolog of MarP does not survive in acidified phagosomes and is unable to successfully establish infection in zebrafish larvae (Levitte *et al*, 2016). This attenuation phenotype underlined the importance of MarP to cope with host-imposed stresses *in vitro* and *in vivo*. However, the mechanisms by which this protease mediates resistance to acidic environments, including the proteolytic substrates of MarP, remained unknown.

Here, we identified RipA—a peptidoglycan hydrolase (Hett *et al*, 2008; Martinelli & Pavelka, 2016)—as a MarP substrate. MarP cleaves RipA and this processing is essential for RipA's activity. Using co-immunoprecipitation, we confirmed that MarP and RipA

¹ Department of Microbiology and Immunology, Weill Cornell Medical College, New York, NY, USA

² Department of Medicine, Weill Cornell Medical College, New York, NY, USA

³ Division of Infectious Diseases, Memorial Sloan Kettering Cancer Center, New York, NY, USA

*Corresponding author. Tel: +646 962 6215; E-mail: sae2004@med.cornell.edu

[†] Present address: Division of Translational Research, Exploratory Oncology Research & Clinical Trial Center, National Cancer Center, Kashiwa, Chiba 277-8577, Japan

interact *in vivo*. Cells lacking MarP or RipA share similar phenotypes; both mutants display increased cell length and form chains when subjected to an acidic condition. Our data suggest that the inability of MarP-deficient cells to survive acidic stress originates from their incapacity to maintain RipA-dependent PG hydrolysis.

Results

MarP-deficient cells elongate during acid stress

First, we determined the impact of pH on the morphology of MarP-deficient mycobacteria because Mtb $\Delta marP$ is hypersensitive to acid (Vandal *et al*, 2008; Biswas *et al*, 2010). We deleted *marP* in *M. smegmatis* (Msm; Appendix Fig S1A and B) and verified that the mutant was hypersensitive to acid (Appendix Fig S1C). We subjected WT, $\Delta marP$, and $\Delta marP::marP$ of Mtb and Msm to minimal media at neutral or acidified pH. Next, we measured the size of bacterial cells along their longitudinal axis. The cell length of Mtb WT and $\Delta marP::marP_{TB}$ cells was similar, either at neutral or at acidic pH. However, Mtb $\Delta marP$ cells elongated when perfused with minimal medium at pH 5 for 7 days (Fig 1A and Appendix Table S1). Although incubation of Msm WT and $\Delta marP::marP_{smeg}$ cells for 24 h at pH 4.5 minimally affected cell length compared to pH 7.2, Msm $\Delta marP$ cells were abnormally long after 24 h of incubation in acidified minimal medium (Fig 1B and Appendix Table S1). Using the supravital fluorescent D-alanine analog NBD-amino-D-alanine (NADA) that incorporated into the peptidoglycan (PG) of bacteria (Fig EV1A, Appendix Fig S2; Kuru *et al*, 2012, 2015), we labeled the septa of all three Msm strains that were incubated at pH 7.2 or pH 4.5 for 24 h. Unlike WT and $\Delta marP::marP_{smeg}$, Msm $\Delta marP$ formed chains at pH 4.5 (Fig 1C). We further quantified the number of septa per bacterium and observed that 33.9% of Msm $\Delta marP$ cells contained at least two septa at pH 4.5, in contrast to only 2.7% and 3.5% for Msm WT and $\Delta marP::marP_{smeg}$, respectively (Fig 1D).

The separation of progeny cells is impaired in Msm MarP-deficient cells at acidic pH

The formation of chains of Msm $\Delta marP$ exposed to acidic medium suggested impaired cell separation. Thus, we evaluated the dynamics of septum formation and separation of a progeny pair during acid challenge. We monitored the formation and resolution of septa in single cells subjected to pH 7.2 and pH 4.5 using NADA and HADA, another fluorescent D-alanine analog (Figs 2A and EV1A; Kuru *et al*, 2015). Bacteria were incubated in regular growth medium containing 1 mM HADA for 4 h. Cells were then washed to remove excess HADA and incubated in Sauton's medium at pH 7.2 or pH 4.5 supplemented with 1 mM NADA (Figs 2B and EV1B). Next, we counted the number of septa per bacterium and we quantified the number of septa labeled with HADA, NADA, or both to determine when the septum had formed. A septum labeled with HADA alone or co-labeled with NADA indicated that it had formed before the switch to Sauton's medium, while labeling with NADA alone indicated that a septum had formed after the switch. Statistical analysis of the data is summarized in Appendix Table S2.

After incubation at pH 7.2 for 4 and 16 h, Msm WT, $\Delta marP$, and $\Delta marP::marP_{smeg}$ contained septa labeled with NADA only (Fig 2C). After 4 h at pH 4.5, all three strains presented almost exclusively septa stained with HADA only or both probes. This suggested that few new septa had formed within the 4 h following the transition to acidic pH and that cells in which septa had appeared prior to transition to acidic pH had an impaired ability to complete separation (Fig 2C). After 16 h at pH 4.5, all three strains presented a large number of cells that contained at least one septum. In $\Delta marP$, 17.4% of the septa remained labeled with HADA, whereas only 5.1 and 6.2% were HADA-labeled in WT and complemented mutant, respectively (Fig 2C). We next looked at the proportion of cells forming chains at acidic pH and we assessed how they were labeled. Only 2.7 and 0.4% of Msm WT and $\Delta marP::marP_{smeg}$ cells formed chains after 16 h at pH 4.5, respectively. In contrast, 15.6% of Msm $\Delta marP$ had multiple septa; 1.2 and 0.4% of Msm WT and $\Delta marP::marP_{smeg}$ septa were labeled with HADA. This number increased to 6.7% in $\Delta marP$ cells (Fig 2D).

Collectively, these results indicated that exposure to acidic stress led to transiently impaired cell separation of a progeny pair. In Msm WT and $\Delta marP::marP_{smeg}$, cell separation was delayed at acidic pH, but eventually sibling cells separated. However, this phenotype was exacerbated in cells lacking MarP, and culminated in the formation of chains, as new septa formed in cells that had not yet completed prior division.

Cell separation is impaired in Mtb $\Delta marP$

Next, we used the D-alanine analogs to study the formation and resolution of septa in Mtb. We incubated Mtb WT, $\Delta marP$, and $\Delta marP::marP_{TB}$ cells in regular growth medium containing 1 mM HADA for 24 h. Cells were washed to remove excess HADA prior to incubation for 16 h in Sauton's medium at pH 7.2 or pH 4.5 supplemented with 1 mM NADA (Fig EV1C). At pH 7.2, the proportion of bacteria that had at least one septum was 10.4% in MarP-deficient Mtb and 3.5 and 4.3% in the WT and complemented strains, respectively (Fig 2E). Almost all septa in Mtb WT and $\Delta marP::marP_{TB}$ were labeled only with NADA, while 40% of septa in MarP-deficient cells were labeled with NADA, 20% with both HADA and NADA, and 40% with HADA only. The proportion of cells bearing a septum increased at pH 4.5 in $\Delta marP$ (22.9%) and no new septa formed, whereas this proportion decreased to 2.7 and 1.7% in Mtb WT and $\Delta marP::marP_{TB}$, respectively, and they were newly formed septa. This suggested that septum resolution was delayed in the absence of MarP at acidic pH, extending the time required for completion of cell separation.

Catalytically inactive MarP-S343A leads to the formation of chains in MarP-deficient cells

MarP consists of four N-terminal transmembrane helices and a serine protease domain that is located in the periplasm (Biswas *et al*, 2010; Small *et al*, 2013). The catalytic amino acid triad His²³⁵, Asp²⁶⁴, and Ser³⁴³ is required for MarP's protease activity (Biswas *et al*, 2010). A Ser³⁴³ to Ala³⁴³ point mutant of MarP (MarP-SA) is catalytically inactive *in vitro* and fails to complement the acid hypersensitivity of $\Delta marP_{TB}$ (Vandal *et al*, 2008; Biswas *et al*, 2010). We transformed Msm and Mtb WT and *marP*-deficient mutants with

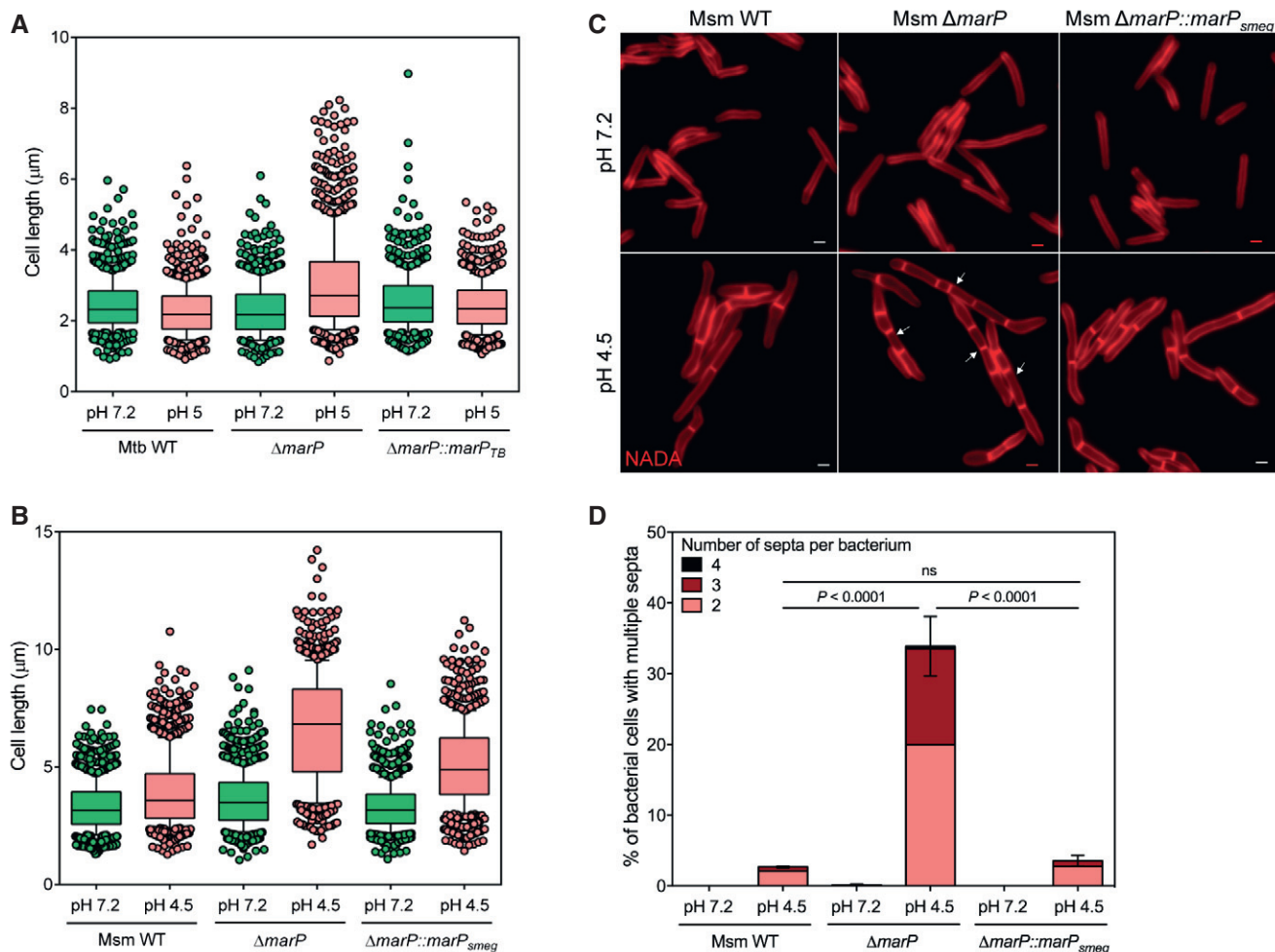


Figure 1. $\Delta marP$ subjected to acidic medium elongates abnormally.

- A** Boxplot of the lengths (μm) of Mtb WT, $\Delta marP$, and $\Delta marP::marP_{TB}$ incubated for 7 days in Sauton's medium at pH 7.2 or pH 5 measured in three independent experiments. Lower and upper whiskers extend to the 10th and 90th percentiles, respectively. The middle bar represents the median and the lower and upper box limits are the 25th and 75th percentiles. For Mtb WT pH 7.2, $n = 186, 343, 351$; pH 5, $n = 298, 278, 238$. For $\Delta marP$ pH 7.2, $n = 210, 183, 422$; pH 5, $n = 180, 419, 365$. For $\Delta marP::marP_{TB}$ pH 7.2, $n = 163, 235, 305$; pH 5, $n = 247, 258, 297$. n indicates the number of cells in experiments 1, 2, and 3. Adjusted P -values compared to WT pH 7.2: $\Delta marP$ pH 7.2, $P = 1$; $\Delta marP::marP_{TB}$ pH 7.2, $P = 5.8 \times 10^{-4}$. Adjusted P -values compared to WT pH 5: $\Delta marP$ pH 5, $P = 1.8 \times 10^{-56}$; $\Delta marP::marP_{TB}$ pH 5, $P = 1.4 \times 10^{-6}$. P -values have been computed using the Ranksum test adjusted for multiple testing.
- B** Boxplot of the lengths (μm) of Msm WT, $\Delta marP$, and $\Delta marP::marP_{smeg}$ incubated for 24 h in Sauton's medium at pH 7.2 or pH 4.5, measured in three independent experiments. Lower and upper whiskers extend to the 10th and 90th percentiles, respectively. The middle bar represents the median and the lower and upper box limits are the 25th and 75th percentiles. For Msm WT pH 7.2, $n = 309, 431, 444$; pH 4.5, $n = 142, 327, 546$. For $\Delta marP$ pH 7.2, $n = 205, 465, 610$; pH 4.5, $n = 259, 268, 279$. For $\Delta marP::marP_{smeg}$ pH 7.2, $n = 249, 464, 577$; pH 4.5, $n = 239, 358, 234$. n indicates the number of cells in experiments 1, 2, and 3. Adjusted P -values compared to WT pH 7.2: $\Delta marP$ pH 7.2, $P = 1.3 \times 10^{-4}$; $\Delta marP::marP_{smeg}$ pH 7.2, $P = 0.22$. Adjusted P -values compared to WT pH 4.5: $\Delta marP$ pH 4.5, $P = 3.3 \times 10^{-124}$; $\Delta marP::marP_{smeg}$ pH 4.5, $P = 4.2 \times 10^{-25}$. P -values have been computed using the Ranksum test adjusted for multiple testing.
- C** Representative images of Msm WT, $\Delta marP$, and $\Delta marP::marP_{TB}$ incubated for 24 h in Sauton's medium at pH 7.2 or pH 4.5 in the presence of 1 mM of the D-alanine analog NADA (red). Arrows show examples of bacteria that formed chains. Scale bars, 1 μm .
- D** Quantification of the number of bacteria that contained at least two septa for Msm WT, $\Delta marP$, and $\Delta marP::marP_{smeg}$ after 24 h of incubation at pH 7.2 or pH 4.5 in three independent experiments. Error bars represent SEM. P -values were determined using a logistic regression model and were adjusted for multiple comparisons.

flag-tagged *marP*-SA. Expression of the inactive mutant protein induced by the addition of anhydrotetracycline (Atc) impaired growth of *marP*-deficient cells at neutral pH (Fig 3A and B, Appendix Fig S3A and B). In Msm $\Delta marP$, the growth defect caused by MarP-S343A expression was associated with elongated cells containing numerous septa (Fig 3C). The toxicity of MarP-S343A in the absence of wild-type MarP suggested that its substrate(s) may be required for optimal separation of dividing cells. This process

requires PG degradation, a reaction catalyzed in mycobacteria by the PG hydrolases RipA and RipB (Hett *et al*, 2008; Martinelli & Pavelka, 2016). Using an Atc-regulated Msm strain, Hett *et al* showed that transcriptional silencing of *ripA*_{smeg} in response to Atc removal is associated with a loss of viability (Hett *et al*, 2008). This phenotype is likely caused by silencing of *ripA*_{smeg} and *ripB*_{smeg}—which is located downstream of *ripA*_{smeg}—as *ripA*_{smeg} has recently been reported to be dispensable for growth if *ripB* is expressed (Hett

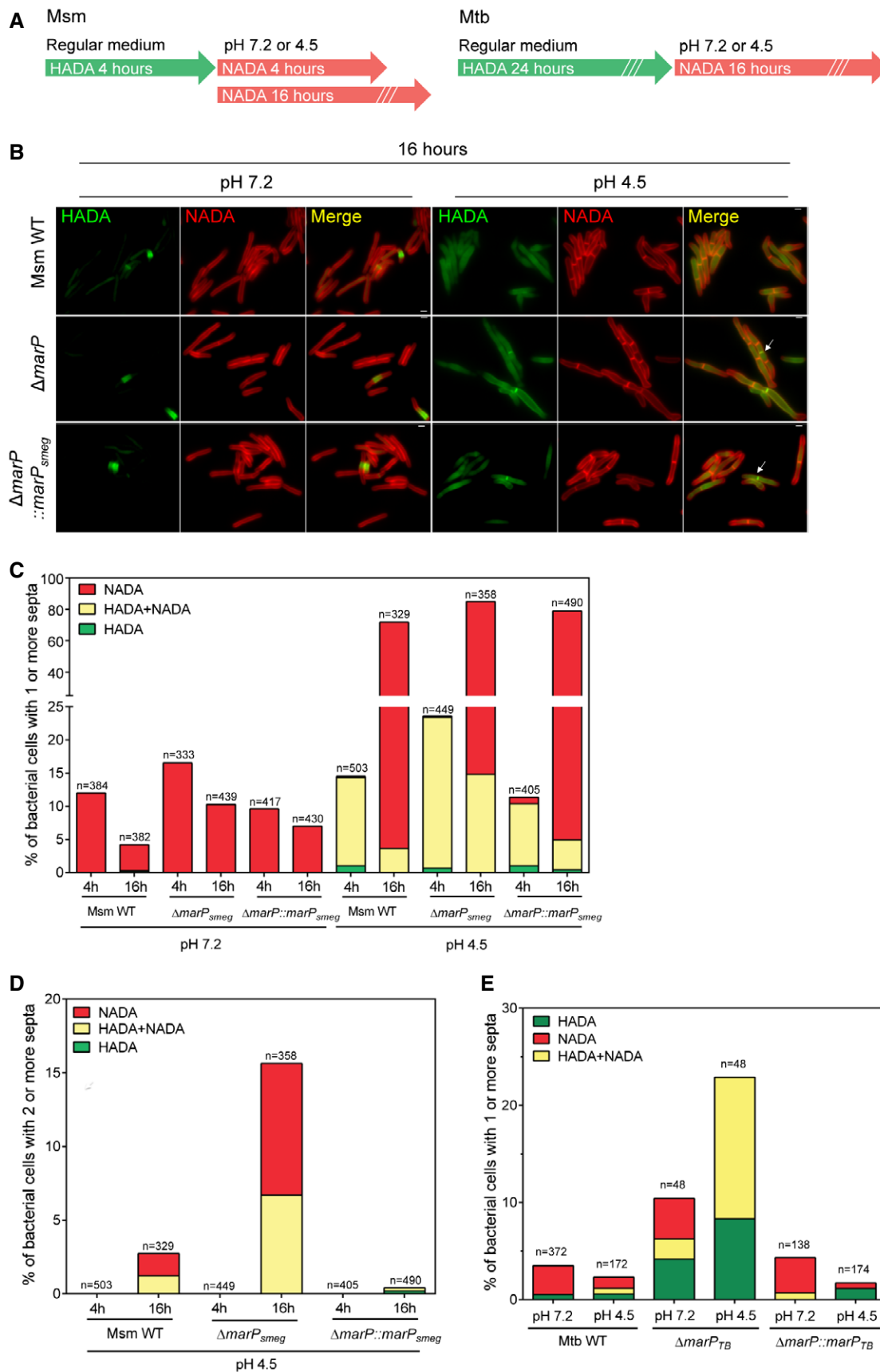


Figure 2.

Figure 2. The separation of progeny cells is impaired in Δ marP mutants during acid stress.

- A Schematic of peptidoglycan labeling experiments for Msm and Mtb.
- B Representative images of Msm WT, Δ marP, and Δ marP::marP_{smeg} incubated in 7H9 medium containing 1 mM HADA for 4 h, washed, and further incubated in Sauton's medium at pH 7.2 or at pH 4.5 containing 1 mM NADA for 16 h. Arrows show examples of septa labeled with both HADA and NADA. Scale bars, 1 μ m. See also Fig EV1B.
- C Proportion of bacteria that contained at least one septum. All septa labeled with HADA only (green), with NADA only (red), or with at least one septum labeled with both probes (yellow) are reported for Msm WT, Δ marP, and Δ marP::marP_{smeg}. The bacteria were incubated in 7H9 medium containing 1 mM HADA for 4 h, washed, and further incubated in Sauton's medium at pH 7.2 or pH 4.5 containing 1 mM NADA for 4 or 16 h.
- D Proportion of bacteria in (C) that contained at least two septa after incubation in Sauton's medium at pH 4.5 for 4 or 16 h. Green, red, and yellow indicate bacteria for which all septa were labeled with HADA only, NADA only, or that had at least one septum labeled with both probes, respectively.
- E Proportion of bacteria with a septum labeled with HADA only (green), NADA only (red), or both HADA and NADA (yellow). Mtb WT, Δ marP, and Δ marP::marP_{TB} cells were incubated in 7H9 medium containing 1 mM HADA for 24 h, washed, and further incubated in Sauton's medium at pH 7.2 or at pH 4.5 containing 1 mM NADA for 16 h. See also Fig EV1C.

Data information: Experiments reported in panels (C, D, and E) are representative of three independent biological replicates. The number of bacteria counted is indicated for each dataset.

et al, 2008; Martinelli & Pavelka, 2016). We further refer to this strain as RipAB knockdown (KD). Of note, this strain forms chains, branches, and bulges in the absence of the inducer, a consequence of defective PG hydrolysis (Hett et al, 2008).

MarP cleaves RipA *in vitro* to release RipA's PG hydrolase domain

RipA possesses a PG hydrolase domain located at its C-terminus and its N-terminal domain is EnvC-like. EnvC is a coil-coiled domain involved in protein–protein interactions critical for cell division (Fig 4A; Uehara et al, 2010; Yang et al, 2011; Peters et al, 2013). Previous studies suggested that RipA needs to be proteolytically processed for optimal PG hydrolase activity (Ruggiero et al, 2010; Chao et al, 2013). Processed forms of RipA have been reported *in vivo* in Msm, but proteases that activate RipA have not been identified (Chao et al, 2013). The phenotypes shared by RipAB KD cells and MarP-deficient cells in acidic medium led us to hypothesize that MarP cleaves and activates RipA at acidic pH.

To test this, we first assessed the ability of MarP to cleave RipA *in vitro*. We purified RipA_{TB} without the signal sequence that targets it to the periplasm and incubated it with the protease domain of MarP_{TB} and MarP-S343A purified as reported (Small et al, 2013). Under conditions that were optimal for its activity (Small et al, 2013), MarP_{TB} cleaved RipA_{TB} into three fragments with approximate molecular weights of 25, 14, and 10 kDa (Fig 4B, black arrows). An intermediate fragment of RipA_{TB} of ~35 kDa was detected after 6 h of incubation prior to further processing into the ~25-kDa and ~10-kDa fragments (Fig 4B, arrowhead). We generated two truncated versions of RipA_{TB} and determined whether MarP_{TB} could process them: RipA-Nter consisting of residues 42 to 235 and RipA-Cter consisting of residues 263 to 472. We observed ~14-kDa and ~10-kDa species of RipA after cleavage of RipA-Nter by MarP_{TB} but no processing of RipA-Cter by MarP_{TB} (Fig EV2). Collectively, this suggests that RipA_{TB} may be cleaved at two different sites by MarP_{TB}, generating fragments of about 25, 14, and 10 kDa. The specificity of the proteolytic event was further evidenced by the failure of MarP_{TB} to process an unrelated enzyme, 1,3-fructose biphosphatase (GlpX), and the inability of MarP-S343A to cleave RipA (Fig 4B).

Using mass spectrometry, we identified the major fragment generated upon MarP_{TB} cleavage. The 25-kDa fragment corresponded to the C-terminus of RipA_{TB} (²³⁶A to ⁴⁷²Q), indicating that MarP_{TB} cleaves RipA_{TB} after valine 235 (Fig 4A, Appendix Fig S4A and B). Peptide substrate profiling had revealed that MarP_{TB} cleaves

preferentially after a residue that is preceded by a leucine or a tryptophan and followed by an alanine or an asparagine (Small et al, 2013). Consistent with this, a leucine (²³⁴Leu) precedes ²³⁵V and an alanine (²³⁶A) follows ²³⁵V. We further introduced the substitutions L234G (RipA-LG) and L234G-V235G (RipA-LGVG) in the amino acid sequence of RipA_{TB}. MarP_{TB} did not effectively process these mutant proteins, as the ~25-kDa fragment of RipA was less abundant after prolonged incubation of MarP_{TB} with either mutant. Moreover, the ~35-kDa fragment appeared more stable when we used the two mutant proteins as substrates of MarP_{TB} (Fig 4C, red arrows). These results confirmed the specificity of MarP_{TB} for the cleavage sequence in RipA_{TB} and identified the MarP_{TB} cleavage site in the N-terminus of RipA_{TB}.

The 25-kDa processed form of RipA contains the peptidoglycan hydrolase domain. We thus hypothesized that the impaired cleavage of RipA-LG and RipA-LGVG by MarP may prevent the release of the active hydrolase domain. Therefore, we sought to determine the biological impact of impaired RipA processing on Msm and Mtb.

RipALG fails to rescue the growth defect of Msm RipAB KD

To test the consequence of the cleavage site mutation on RipA's activity *in vivo*, we monitored the ability of RipA-LG to phenotypically complement the RipAB KD after Atc was removed. To do so, we constitutively expressed RipA_{TB} and RipA-LG fused to an HA tag in Msm RipAB KD and monitored the growth of colonies on agar plate deprived of Atc. RipA_{TB}, but not RipA-LG, allowed the growth of RipAB KD without the inducer (Fig 4D). Western blot analysis verified that both RipA_{TB} and RipA-LG were expressed in Msm RipAB KD (Appendix Fig S4C). Finally, we inspected by photomicroscopy the morphology of Msm RipAB KD and Msm RipAB KD expressing RipA_{TB} or RipA-LG incubated in the absence of Atc. As expected, while constitutive expression of functional RipA (RipA_{TB}) resulted in wild-type morphology, expression of RipA-LG led to chaining, bulging, and branching, as documented for the RipAB KD (Hett et al, 2008; Fig 4E). Altogether, these results suggest that RipA's activity *in vivo* required its cleavage at a site that is recognized by the protease MarP.

RipA_{TB} and MarP_{TB} interact in acid-stressed cells

Because GFP is prone to unfolding and degradation when expressed in the periplasm, we codon-adapted a superfolder GFP (sfGFP) and

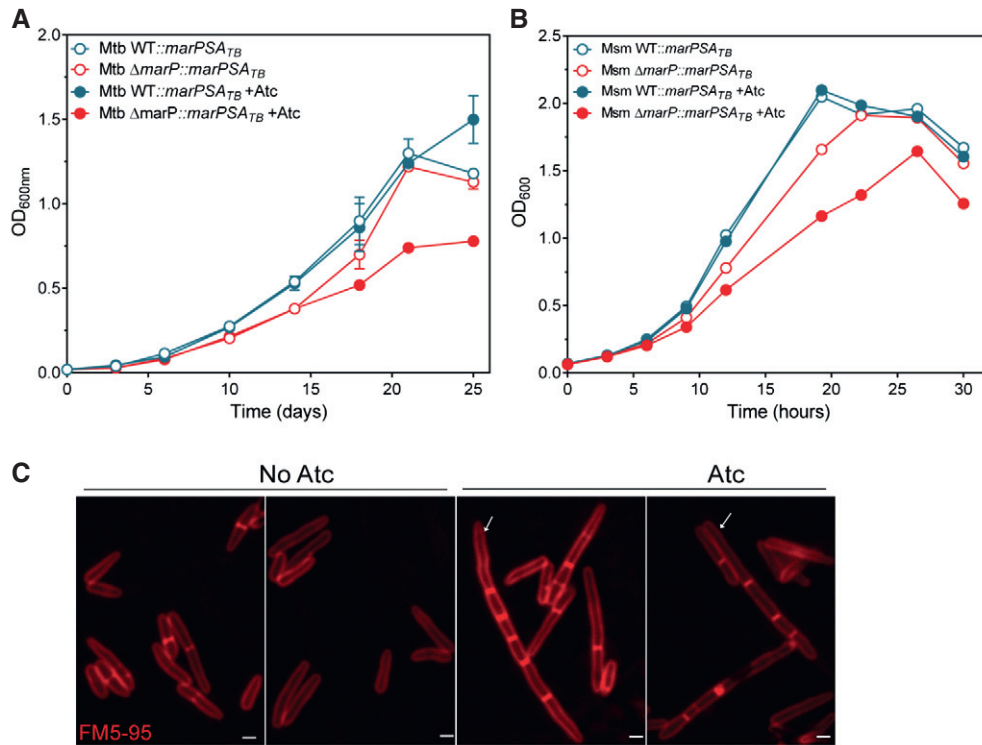


Figure 3. Expression of catalytically inactive MarP5343A in MarP-deficient cells impairs growth and causes the formation of chains.

A Mtb growth curve in Sauton's medium at pH 7.2. Mtb WT and $\Delta marP$ expressing *marP5343A* from an Atc-inducible promoter; 1 μ g/ml of Atc was added at day 6 (closed symbols). Data are means of triplicate cultures and error bars represent SD.

B Growth of Msm in 7H9 medium. Msm WT and $\Delta marP$ expressing *marP5343A* from an Atc-inducible promoter; 200 ng/ml of Atc was added after 3 h of incubation (closed symbols).

C Representative images of Msm $\Delta marP$ expressing *marP5343A* from an Atc-inducible promoter, with no Atc (2 panels on the left) or 200 ng/ml of Atc (2 panels on the right). Arrows show examples of bacteria that formed chains. Scale bars, 1 μ m.

Data information: Data in panels (A, B, and C) are representative of three independent experiments. See also Appendix Fig S3.

fused it to MarP_{TB} (Pédélecq *et al*, 2006). We co-expressed MarP_{TB}-GFP_{SF} and RipA_{TB}-HA in Msm $\Delta marP$. Whole-cell lysates were extracted after 4 h of incubation in minimal medium at pH 4.5 and MarP_{TB}-sfGFP was immunoprecipitated using anti-GFP-coated magnetic beads. A strain that expressed sfGFP instead of MarP_{TB}-sfGFP served as a negative control. Using an anti-HA antibody, we detected different forms of RipA_{TB} in Msm protein lysates (Fig 5, second panel); the strongest signal was attributed to the full-length RipA_{TB} (Fig 5, blue arrow). Full-length RipA_{TB} was also present in the MarP_{TB}-sfGFP eluate, but not in the sfGFP eluate, indicating that RipA_{TB} co-immunoprecipitated with MarP_{TB} (Fig 5, fourth panel). To determine whether MarP and RipA specifically interact at acidic pH, we immunoprecipitated MarP_{TB}-sfGFP after cells were incubated at acidic or neutral pH. A greater amount of RipA_{TB}-HA co-immunoprecipitated with MarP_{TB}-sfGFP when cells were subjected to pH 4.5 compared to pH 7.2 (Fig EV3). We conclude that RipA_{TB} and MarP_{TB} chiefly interact *in vivo* when cells are exposed to acidic pH.

RipA is essential for cell separation during acid stress

If the protease MarP activates RipA at acidic pH, we hypothesized that a RipA mutant must recapitulate the phenotype of

MarP-deficient cells perfused with acidic medium. To test this, we incubated Msm WT, $\Delta ripA$, and $\Delta ripA/ripA_{smeg}$ (Martinelli & Pavelka, 2016) in Sauton's medium at pH 7.2 or pH 4.5 supplemented with 1 mM NADA for 24 h. At pH 7.2, the length distribution of the bacterial cells was similar for the three strains, whereas a significant number of $\Delta ripA$ cells were longer at pH 4.5 compared to Msm WT and $\Delta ripA/ripA_{smeg}$ (Fig 6A and Appendix Table S3). We counted the number of bacteria containing more than two septa (Fig 6B and C). Only 2.4 and 4.1% of WT and complemented cells, respectively, presented multiple septa at pH 4.5. In contrast, 19% of $\Delta ripA$ cells formed chains, indicating that RipA's activity is essential in acidic environment to mediate cell separation.

Discussion

Many bacteria face acidic environments within their ecological niche or during their infectious cycle and have evolved mechanisms to withstand this stress (reviewed in Foster, 2004; Krulwich *et al*, 2011; De Biase & Lund, 2015). For example, *Escherichia coli* (*E. coli*) uses amino acid decarboxylase/antiporter systems that utilize glutamate, arginine, and lysine as substrates to increase its cytoplasmic pH (Lin *et al*, 1995; Foster, 2004). Additionally, the periplasmic

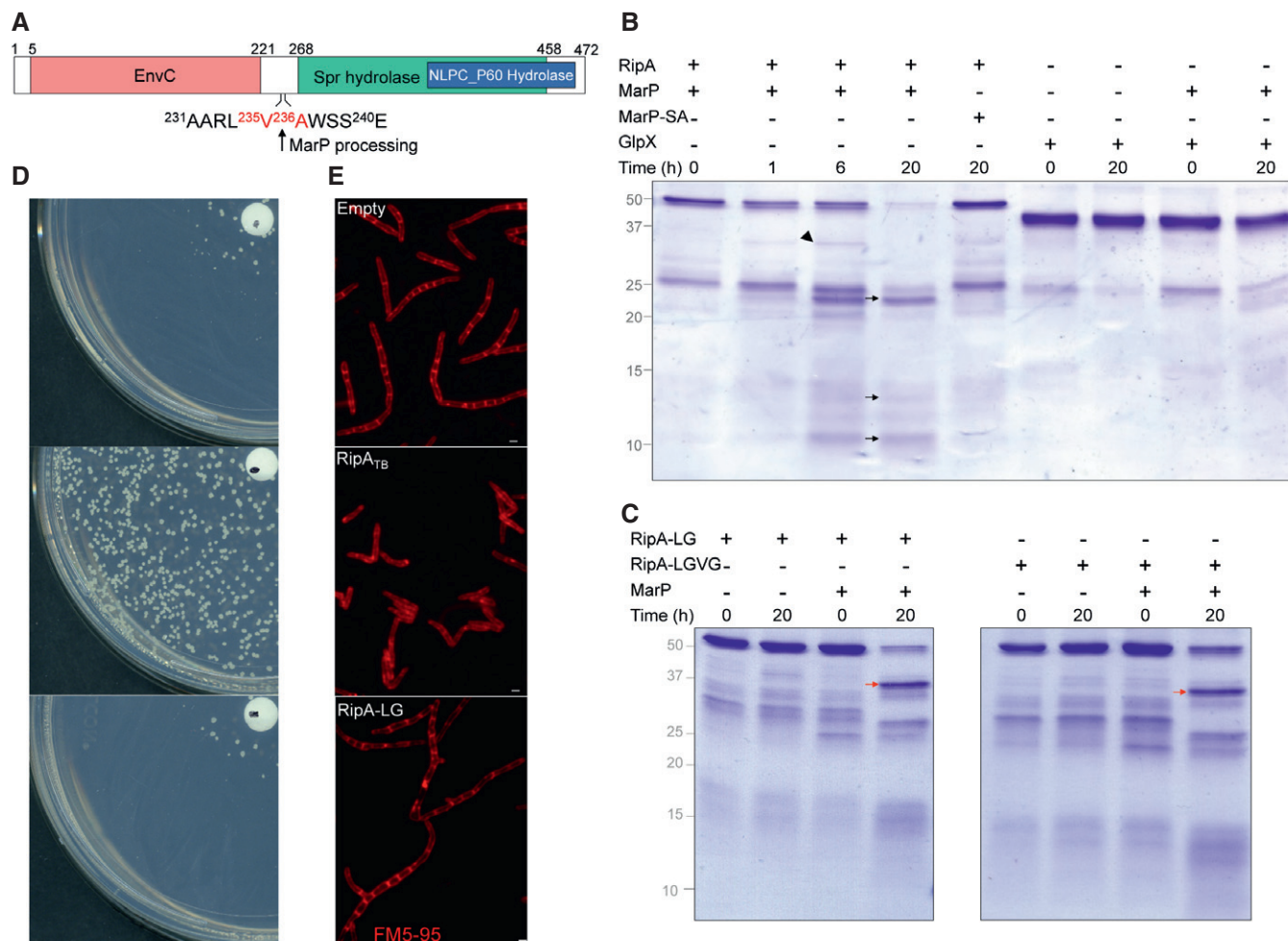


Figure 4. MarP cleaves RipA *in vitro* and mutation of the cleavage site inhibits RipA activity *in vivo*.

- A** Schematic of RipA representing its domains predicted by BLASTP (<https://blast.ncbi.nlm.nih.gov/>). The amino acid sequence of the region where MarP cleaves RipA is indicated. MarP cleaves between the two residues shown in red.
- B, C** 10 μ g of RipA (B), RipA-LG, or RipA-LGVG (C) was incubated with 1 μ g of MarP or MarP-S343A at 37°C. Reactions were run on SDS-PAGE and gels were stained with Coomassie blue. Size of uncleaved RipA, RipA-LG, and RipA-LGVG: 49 kDa, size of MarP_{179–397}: 24 kDa. Arrowhead points to the partially processed form of RipA. Black arrows point to the fully processed forms of RipA. Red arrows point to incompletely processed RipA.
- D** Msm RipAB knockdown transformed with an empty plasmid, a plasmid encoding RipA_{TB}, or RipA-LG expressed from a constitutive promoter was plated on 7H10 plates. The disk in the center of the plate contains 50 ng of Atc; the concentration of Atc decreases from the center to the periphery of the plate.
- E** Micrographs of Msm RipAB KD-empty, RipAB KD-RipA_{TB}, RipAB KD-RipA-LG incubated for 24 h in 7H9 medium without Atc. Membranes were stained with FM5-95 (red). Scale bars, 1 μ m.

Data information: Data in panels (B–E) are representative of three independent experiments. See also Appendix Fig S4.

chaperones HdeA and HdeB, and the cytoplasmic chaperone Hsp31, help preserve protein structure and activity in acidic conditions and the nucleoid binding protein Dps maintains DNA integrity (Choi *et al*, 2000; Gajiwala & Burley, 2000; Mujacic & Baneyx, 2007). Mechanisms in other microorganisms include the modification of the cell envelope, the formation of biofilms, the hydrolysis of ATP by the F₁F₀ ATPase, the activation of K⁺Na⁺/H⁺ antiporters, or the production of molecules with alkali power (Kullen & Klaenhammer, 1999; Li *et al*, 2001; Martín-Galiano *et al*, 2001; Wen & Burne, 2004; Kim *et al*, 2005; Maroncle *et al*, 2006; Shabala & Ross, 2008; Williams & Cámara, 2009).

Mtb limits its exposure to acidic pH in infected hosts by blocking the fusion of the phagosome with lysosomes. If halting phagosomal

maturation fails, Mtb possesses mechanisms by which it can survive in acidified phagosomes. Several proteins have been implicated in Mtb's adaptation to acid stress, such as the two-component system PhoP/PhoR and the outer membrane protein OmpATB (Walters *et al*, 2006; Abramovitch *et al*, 2011; Song *et al*, 2011; Baker *et al*, 2014). A screen of an Mtb transposon mutant library for genes controlling Mtb's ability to survive a 6-day exposure to pH 4.5 identified the periplasmic protease MarP as essential to resist acid stress (Vandal *et al*, 2008). In the absence of MarP, Mtb cannot maintain a neutral intracellular pH and dies *in vitro* at pH 4.5 and in activated macrophages (Vandal *et al*, 2008). The molecular mechanisms by which MarP protects mycobacteria against acid stress remain to be elucidated.

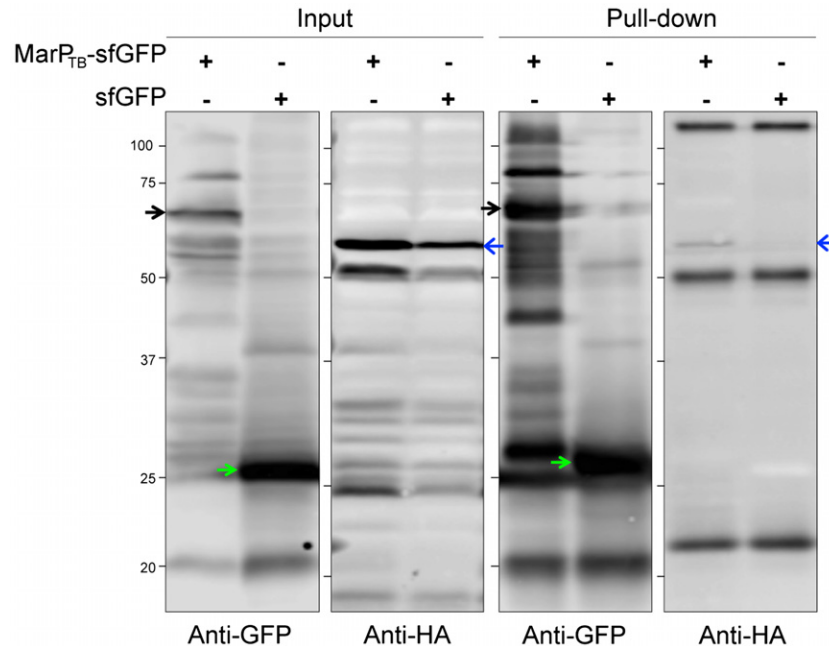


Figure 5. RipA_{TB} and MarP_{TB} interact *in vivo*.

Co-immunoprecipitation of RipA_{TB} and MarP_{TB} from whole-cell protein lysates of *Msm* $\Delta marP::MarP_{TB}\text{-sfGFP}::RipA_{TB}\text{-HA}$ incubated for 4 h at pH 4.5. Whole-cell protein lysates of *Msm* $\Delta marP::sfGFP::RipA_{TB}\text{-HA}$ cells served as a control. MarP-sfGFP_{SF} and sfGFP were pulled down using anti-GFP-coated magnetic beads. Whole-cell lysates (input) and GFP eluates (pull-down) were analyzed by SDS-PAGE, and MarP_{TB}-sfGFP (black arrows), sfGFP (green arrows), and RipA_{TB}-HA (full-length RipA, blue arrows) were detected by Western blot using anti-GFP or anti-HA antibodies. Data are representative of three independent experiments.

Source data are available online for this figure.

Here, we report that exposure of *Mtb* and *Msm* lacking MarP to an acidic medium resulted in significant cell elongation and led to a large increase in the proportion of cells containing one or more septa. These phenotypes may originate from an overall reduction in cell division processes combined with impaired cell separation. The labeling of nearly all septa after 4 h at pH 4.5 with D-alanine analogs with which cells were pulsed prior to the switch to acidic pH supports this hypothesis and excludes that cell division was promoted. The effect of acid stress on cell separation was exacerbated in the mutant resulting in chain formation. Collectively, these results suggested that MarP plays a role in cell separation when cells are subjected to acid stress (Fig 7).

Cell separation requires the coordinated activities of lytic transglycosylases, amidases, and PG-cleaving endopeptidases (Typas *et al*, 2012). In mycobacteria, the endopeptidase RipA has been shown to be important for cell separation, as *Msm* cells in which *ripA* expression was repressed failed to complete separation and formed chains (Hett *et al*, 2008). However, a recent study has reported that the silencing of *ripA* affects the expression of the downstream gene *ripB* (Martinelli & Pavelka, 2016). RipB is homologous to the C-terminal amino acid sequence of RipA, which comprises the PG hydrolysis activity domain (NLPC_P60 hydrolase) and possesses PG hydrolysis activity (Böth *et al*, 2011). Hence, it is very likely that the phenotype of the RipA KD in Hett *et al*, dubbed in this study RipAB KD, was caused by a polar effect on *ripB* when *ripA* was inactivated. This implies that RipA and RipB have redundant activities and that maintaining the activity of at least one peptidoglycan hydrolase is indispensable for cell

viability. Indeed, the in-frame deletion of *ripA* alone did not lead to the death of *Msm* cells, although they were hypersensitive to vancomycin, erythromycin, rifampin, and detergents (Martinelli & Pavelka, 2016). Interestingly, $\Delta marP$ is similarly hypersensitive to antibiotics that target PG homeostasis—vancomycin and faropenem (Appendix Table S4)—and also to erythromycin, rifampin, and detergent (Vandal *et al*, 2008).

RipA and RipB may also have unique properties, as *ripB* expression rescued the impact of *ripA* deletion on antibiotic and detergent-induced stresses partially (Martinelli & Pavelka, 2016). This might be explained by the presence of additional domains in RipA, and potentially different interacting partners. Indeed, the C-terminal domain of RipA binds other proteins that modify PG, such as RpfB and PBP1. These interactions modulate its hydrolase activity (Hett *et al*, 2007, 2008, 2010). Moreover, processed forms of RipA have been detected in *Msm in vivo*, and it has been shown that proteolytic activation was required to activate RipA (Ruggiero *et al*, 2010; Chao *et al*, 2013). The protease remained to be identified. The nature of the RipA fragment that has optimal PG hydrolase activity is unknown; *in vitro* studies had led to conflicting results that may originate from the sources of PG substrates used in those studies (Ruggiero *et al*, 2010; Böth *et al*, 2011). The hydrolytic activity on the PG from *Bacillus subtilis* of a RipA fragment containing only the NLPC_P60 domain (residues 332–472) and a larger fragment (residues 263–472) encompassing a loop prone to cleavage was similar (Ruggiero *et al*, 2010). The RipA fragment released by the periplasmic protease MarP (residues 236–472) is similar to the latter. Thus, MarP either releases a 236-amino acid

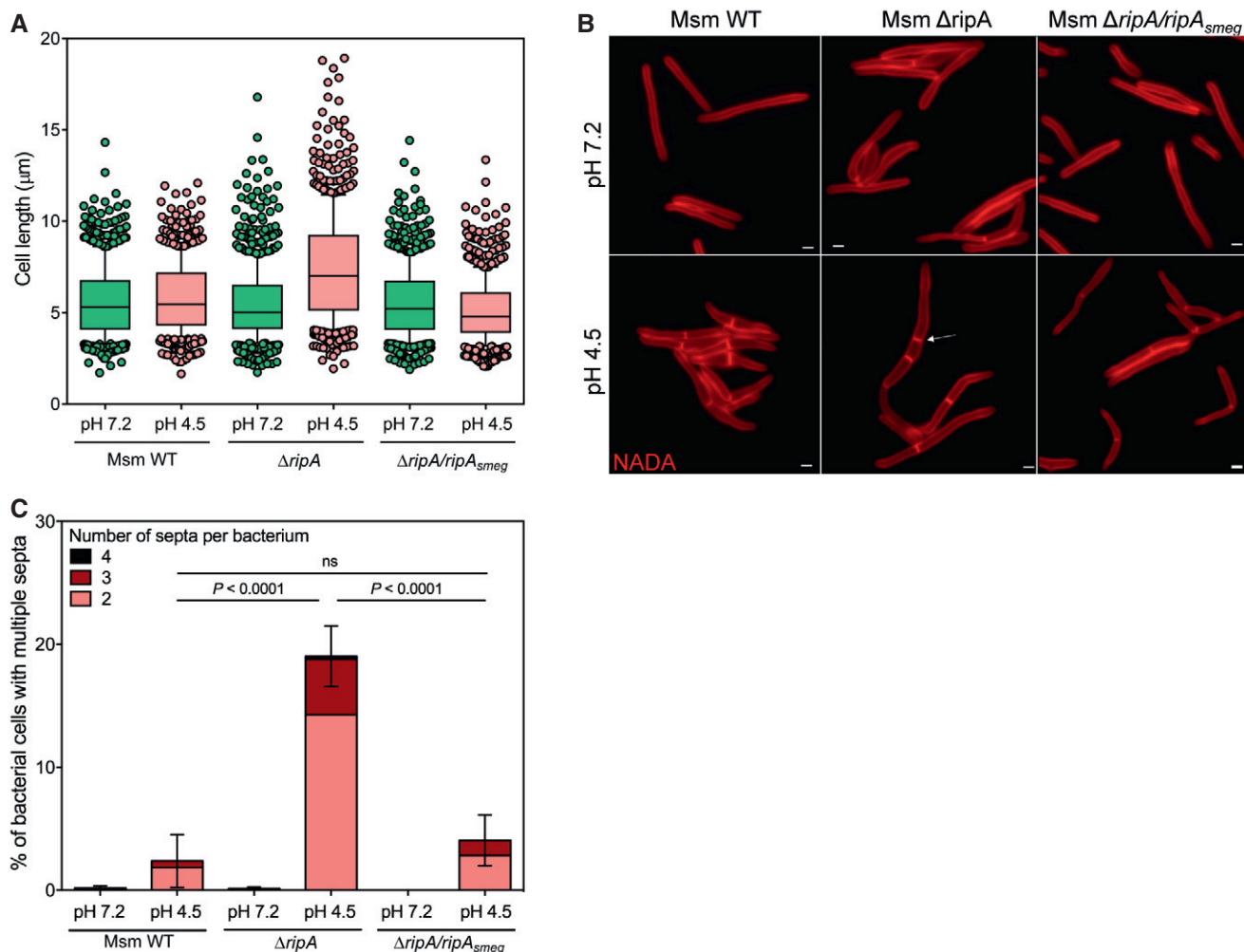


Figure 6. Msm $\Delta ripA$ forms chains during acidic stress.

- A** Boxplot of the lengths (μm) of Msm WT, $\Delta ripA$, and $\Delta ripA/ripA_{smeg}$ incubated for 24 h in Sauton's medium at pH 7.2 or pH 4.5, measured in three independent experiments. Lower and upper whiskers extend to the 10th and 90th percentiles, respectively. The middle bar represents the median and the lower and upper box limits are the 25th and 75th percentiles. The *P*-values have been computed using the Ranksum test adjusted for multiple testing. For Msm WT pH 7.2, *n* = 335, 213, 202; pH 4.5, *n* = 395, 216, 180. For $\Delta ripA$ pH 7.2, *n* = 367, 214, 207; pH 4.5, *n* = 404, 149, 113. For $\Delta ripA/ripA_{smeg}$ pH 7.2, *n* = 323, 281, 181; pH 4.5, *n* = 350, 186, 192. *n* indicates the number of cells in experiments 1, 2, and 3. Adjusted *P*-values compared to WT pH 7.2: $\Delta ripA$ pH 7.2 *P* = 8.4×10^{-5} ; $\Delta ripA/ripA_{smeg}$ pH 7.2, *P* = 6.7×10^{-3} . Adjusted *P*-values compared to WT pH 4.5: $\Delta ripA$ pH 4.5, *P* = 1.3×10^{-15} ; $\Delta ripA/ripA_{smeg}$ pH 4.5, *P* = 7.7×10^{-4} .
- B** Representative images of Msm WT, $\Delta ripA$, and $\Delta ripA/ripA_{smeg}$ incubated in Sauton's medium at pH 7.2 or at pH 4.5 containing 1 mM NADA for 24 h. Arrows show examples of bacteria that formed chains. Scale bars, 1 μm.
- C** Quantification of the number of bacteria presenting two, three or four septa for Msm WT, $\Delta ripA$, and $\Delta ripA/ripA_{smeg}$ after 24-h incubation at pH 7.2 or pH 4.5 from three independent experiments. Error bars represent SEM. *P*-values were determined using a logistic regression model and adjusted for multiple comparisons.

fragment that possesses PG hydrolysis activity or MarP matures pre-pro-RipA into pro-RipA, the aforementioned 236-amino acid fragment, exposing a second cleavage site in the loop for other proteases.

The inability of RipA_{LG} that cannot be cleaved by MarP to complement RipA and RipB depletion in Msm implies that processing of RipA at the amino acid sequence that is recognized by the protease MarP is essential for its activity. Moreover, RipA and MarP are essential for the separation of progeny cells in acidic medium and the two proteins interact *in vivo* in acidic conditions. Collectively, these results suggest that MarP activates RipA to mediate PG hydrolysis at low pH. The enhanced interaction between MarP and RipA at acidic pH may depend on post-translational modifications of either or both

proteins, as both proteins were constitutively expressed in our experimental system. At neutral pH, MarP might be inhibited and other proteases may regulate RipA. In agreement with this, a benzoxazinone was shown to inhibit MarP and also bind the periplasmic protease and chaperone HtrA1 (Zhao *et al.*, 2015). Moreover, RipB is sufficient to ensure cell separation in rich medium at neutral pH in *M. smegmatis* (Martinelli & Pavelka, 2016).

So far, two other PG-hydrolyzing enzymes have been described to be regulated by proteolytic processing. The N-acetylglucosaminidase Auto, essential for *Listeria monocytogenes* entry into host cells, requires proteolytic cleavage by an unidentified protease (Bublitz *et al.*, 2009). Additionally, the activity of the D, D-endopeptidase MepS from *E. coli* is modulated by the periplasmic protease Prc

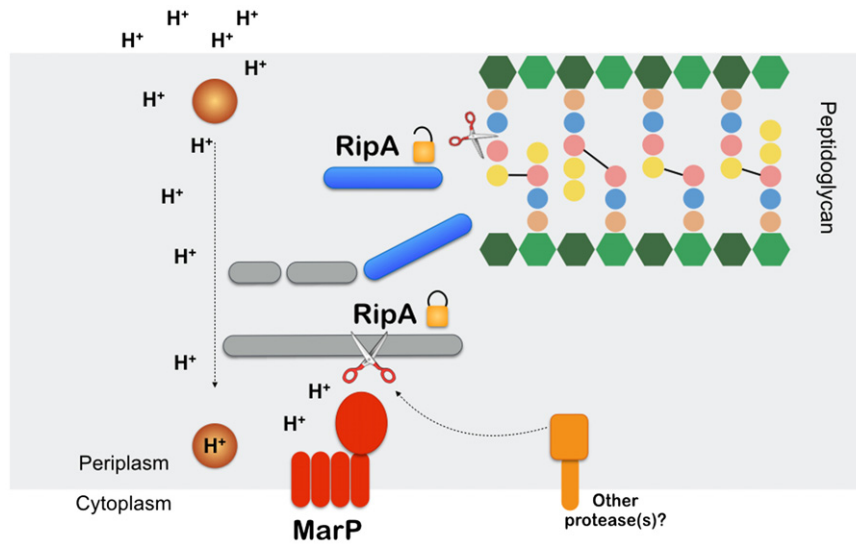


Figure 7. Model for the activation of RipA-mediated PG hydrolysis by MarP in acid-stressed Mtb.

When Mtb faces an acidic environment, the periplasmic protease MarP (red) may sense the stress. Alternatively, MarP might be activated by an unknown protein (brown circle) that senses pH reduction. MarP cleaves the inactive full-length RipA (gray). RipA processing leads to the release of its C-terminal fragment that contains a PG hydrolase domain (blue). In other conditions, other proteases (orange) may activate RipA. Ultimately, PG hydrolysis by activated RipA mediates PG remodeling and/or separation of the progeny pair, processes that may sustain Mtb's survival when subjected to acid stress.

(Singh *et al*, 2015). However, unlike the action of MarP on RipA, PrC controls the level of MepS in *E. coli* by degrading it when it is no longer needed, such as in stationary phase. Thus, our study provides a unique example of a protease that activates a PG-degrading enzyme by proteolytic cleavage.

Our results suggest that sustaining PG hydrolysis may be essential to Mtb's survival in acidic conditions, a stress that it faces in mature phagosomes. Further work will aim to determine whether RipA's activity during acid exposure helps maintain cell division or mediates PG remodeling. Assuring a few rounds of replication events subsequently to stress exposure may be a form of altruism evolved by Mtb to increase cell density and form bacterial structures so that bacilli at the periphery will protect the ones in the center from a stress (Davis *et al*, 2015). Alternatively, it may favor bet-hedging by permitting the distribution of damaged macromolecules between progeny cells so that some sub-population with altered fitness can better adapt to the stress (Manina *et al*, 2015; Vaubourgeix *et al*, 2015). Finally, activation of RipA by MarP may assure PG remodeling, rearrangement, or repair, all of which may be vital to Mtb's survival during stress.

Materials and Methods

Bacterial strains and culture conditions

Strains were cultured at 37°C in Middlebrook 7H9 medium with 0.2% glycerol, 0.5% bovine serum albumin fraction V, 0.05% Tween 80, 0.2% dextrose, 0.085% NaCl, and 0.02% tyloxapol, or Sauton's base medium (0.05% potassium phosphate monobasic, 0.05% magnesium sulfate heptahydrate, 0.2% citric acid, 0.005% ferric ammonium citrate, 0.05% ammonium sulfate, 0.2% glycerol,

0.0001% zinc sulfate, and 0.02% tyloxapol) with the pH adjusted as indicated. For pH 7.2, 0.1 mM MOPS (3-(*N*-morpholino)propanesulfonic acid) was added. For pH 5 and pH 4.5, 0.1 mM MES (2-(*N*-morpholino)ethanesulfonic acid) was added. Strains bearing antibiotic cassettes were cultured with hygromycin (50 µg/ml), zeocin (25 µg/ml), or streptomycin (25 µg/ml). For solid media, Middlebrook 7H11 media with 0.5% glycerol and 10% Middlebrook OADC supplement (final concentration of 0.5% bovine serum albumin fraction V, 0.2% glucose, 0.085% NaCl, 0.006% oleic acid, 0.0003% catalase) were used. For the Msm $\Delta ripA$, $\Delta ripA/ripA_{smeg}$ and the WT counterpart, liquid and solid media were supplemented with 40 µg/ml of L-lysine (Martinelli & Pavelka, 2016).

Construction of expression vectors for MarP_{TB}-Flag, MarP_{SA}-Flag, MarP_{TB}-GFP_{SF}, RipA_{TB}-HA, and RipA_{LC}-HA

Plasmids were constructed using Gateway® Cloning Technology (Life Technologies). sfGFP was codon-adapted to mycobacterial codon usage with the Codon Adaptation Tool at www.jcat.de, synthesized, and cloned into a pUC57 vector (BioBasics). sfGFP was amplified by PCR using primers containing a sequence encoding the linker SGSGSG for the forward primer (*linker-GFP* 5'-tcg ggctcgggctcgggctcgaagggcgaggagctgttcaccgg-3') and the attB3 site for the reverse primer (*GFP-attB3r* 5'-ggggacaacttgtataataaagtgtctactgtacagctcgtccatgcc-3'). The sequence encoding MarP was amplified from Mtb chromosomal DNA with primers allowing addition of the attB2 site upstream (*marP-attB2* 5'-ggggacagcttctgtacaagtggcagaaaggaggttaataatgaccccgctcgcagtgctggatcg-3') and the sequence encoding the linker downstream (*marP-linker* 5'-gcccgagcccagccc gagctgacgcaggcccgggtgccgaccg-3'). A third PCR using these two fragments as templates and marP-attB2 and GFP-attB3 as primers generated a sequence encoding a fusion protein MarP-sfGFP that was

inserted in an episomal expression plasmid under the constitutive *ptb38* promoter. A C-terminal flag tag (DYKDDDDK) was introduced by PCR after *MarP_{TB}* and *MarPS343A* coding sequence without their stop codon using the primers *marP-attB2*, *marP-Flag-Rv* (5'-acttatcgtcatcgtcctttagctgctgacgcaggccccgggcccacc-3'), then *attB3-Flag-Rv* (5'-gggacaactttgtataataaagtttcactatcgtcctttagctg-3'). These coding sequences were then inserted after an *Atc*-inducible promoter (T10-P1) in an episomal plasmid. *RipA_{TB}* and *RipA-HA* were amplified from *Mtb* DNA using primers containing *attB* sites (*ripA-attB2*, 5'-ggggacagcttctgtacaagtgccacagaaaggaggtaataatgacggaatccctggctgcc-3'; *RipA-attB3r*, 5'-ggggacaactttgtataataaagttgtctagctactgtagtccggac-3'; or *ripA-HA-attB3r* 5'-ggggacaactttgtataataaagttgtctagtagcagtagtccggagcgtacatagtagtactgtagtaccgaccacatacg-3'). The LG mutation was introduced in *RipA* coding sequence using primers coding for the mutation (*ripA-LG-Fd* 5'-aggcggccagggcgctgctgg-3' and *ripA-LG-Rv* 5'-aggaccaggaacgcccctggc-3'). *RipA_{TB}*, *RipA-HA*, and *RipALG-HA* sequences were cloned under the *ptb38* promoter in chromosomal expression plasmids that integrate in the *Tweety* site of the mycobacterial chromosome (Pham *et al*, 2007).

Confocal fluorescence microscopy

For length measurements, *Mtb* and *Msm* cultures were inoculated at OD_{600} 0.3 in Sauton's media adjusted at indicated pHs. For growth curve experiments, *Mtb* cultures were inoculated at OD_{600} 0.01 and *Msm* cultures at OD_{600} 0.05. At indicated time points, aliquots were removed and washed once with PBS–0.05% Tween 80. *Mtb* strains were fixed with 4% paraformaldehyde for 4 h before removing from BSL-3 containment. For PG labeling, 1 mM HADA or 1 mM NADA was added to the culture when indicated. Aliquots were removed, washed three times with PBS–0.05% Tween 80, and then fixed with 4% paraformaldehyde for 30 min for *Msm* and 4 h for *Mtb*. Bacterial suspensions were then spread on agar pad and visualized using an inverted Olympus IX-70 microscope equipped with appropriate filter sets, a Photometrics CoolSnap QE cooled CCD camera, and an Insight SSI 7 color solid-state illumination system.

Images were analyzed using ImageJ and the open source image analysis software Icy (Ting *et al*, 1999).

PG labeling probes synthesis

The PG labeling probes HCC-amino-D-alanine (HADA) and NBD-amino-D-alanine (NADA) were synthesized following the procedure described by Kuru *et al* (2015).

Overexpression and purification of *RipA_{TB}*, *RipA-Nter*, *RipA-Cter*, *RipA-LG*, and *RipA-LGVG*

RipA_{TB} (from ⁴²Q to ⁴⁷²Y), *RipA-Nter* (from ⁴²Q to ²³⁵V), and *RipA-Cter* (from ²³⁵V to ⁴⁷²Y) were amplified by PCR from *M. tuberculosis* genomic DNA and mutations were generated by PCR to amplify *RipALG* (²³⁴L to G), *RipALGVG* (²³⁴L to G and ²³⁵V to G) using the primers *ripA-LG-Fd* and *ripA-LG-Rv*, and *ripA-LGVG-Fd* (5'-gcaggcggcagggggcggcct) and *ripA-LGVG-Rv* (5'-tccgaggaccagggcggcggcctgg). The fragments were cloned into pET300/NT-DEST (Invitrogen) using Gateway Cloning Technology. The resulting vectors allowed isopropyl-D-1-thiogalactopyranoside (IPTG)-inducible expression of N-terminal 6×His-tagged proteins in *E. coli* BL21 (DE3) (Invitrogen).

Expression of the proteins was induced with 0.5 mM IPTG at 30°C for 6 h. Cultures were then centrifuged at 4,000 g for 20 min at 4°C. Cell pellets were washed once in 15 ml buffer A (20 mM Tris–HCl, 500 mM NaCl, 25 mM imidazole) and then resuspended in buffer A supplemented with 0.5 μg of lysozyme and 5 μl of DNase I (Invitrogen) and incubated for 30 min at 4°C. The suspension was then subjected to sonication on ice using a Virtis Virsonic 600 sonicator (output setting 6, eight 10-s pulses with 20-s breaks) and centrifuged at 13,000 g for 20 min at 4°C to remove cell debris. The supernatant was clarified using a 0.45-μm PVDF filter. A His Trap HP 5-ml column (GE Healthcare) was equilibrated with 1 column volume of buffer A, loaded with lysate, and then washed with 20 column volumes (100 ml) of buffer A. His-tagged proteins were eluted from the column using a gradient of imidazole from 25 to 500 mM in buffer A. Purity of the sample was assessed by SDS–PAGE. The fractions containing the protein were pooled and concentrated using Amicon Ultra centrifugal devices (Millipore). The sample was dialyzed against buffer A without imidazole using Thermo Slide-A-Lyzer Cassette (12 ml capacity, 10-kDa cutoff). Part of the final sample was stored with 50% glycerol at –20°C for use in *in vitro* cleavage assay or flash-frozen with liquid nitrogen and stored at –80°C for use in antibody generation.

In vitro cleavage assay

1 μg of *MarP*₁₇₉₋₃₉₇ was incubated for 10 min at 37°C in 50 mM Tris, 0.5 M NaCl, 0.01% Triton X-100, pH 7.4; 10 μg of *RipA_{TB}*, *RipA-Nter*, *RipA-Cter*, *RipA_{LG}*, *RipA_{LGVG}*, or *GlpX* was added and further incubated at 37°C for the indicated times. Reactions were stopped by adding SDS sample buffer (2% SDS, 2 mM β-mercapto-phenol, 4% glycerol, 40 mM Tris–HCl, pH 6.8, 0.01% bromophenol blue) and boiling for 10 min.

Immunoprecipitation of sfGFP and *MarP*-sfGFP

Cultures were washed twice with lysis buffer (50 mM Tris–HCl pH 7.4, 50 mM NaCl) containing protease inhibitor cocktail (Roche) and then resuspended in lysis buffer at a ratio of 1 ml/g of pellet. The cells were broken by bead beating (Precellys[®]24, Bertin Technologies or Mini-Beadbeater-1, Bio Spec Products Inc.) and 1% dodecyl maltoside was added. The lysates were incubated for 2 h on ice. Beads were removed by centrifugation for 15 s at 7,500 g and unbroken cells were removed by centrifugation for 5 min at 7,500 g; 5–10 mg of total proteins in lysate was incubated with 30 μl of anti-GFP mAb-magnetic beads (MBL) at 4°C under gentle shaking. After overnight incubation, the supernatant was removed using a DynaMag-Magnet 2 rack (Thermo Fisher scientific). The samples were centrifuged for 30 s at 5000 g to remove the supernatant and then washed three times with PBS. Proteins bound to the beads were then eluted by boiling for 10 min in SDS sample buffer.

MIC determinations

Minimum inhibitory concentrations for the various *Mtb* strains were determined using the microbroth dilution technique—briefly, *Mtb* was grown to mid-log-phase and diluted to an OD_{600} of 0.05. Equal volumes of the suspension were dispensed into a twofold antibiotic dilution series in Middlebrook 7H9 media to a final OD_{600} of 0.025

per well. Optical density was measured after 10 days of outgrowth, and the minimum inhibitory concentration was defined to be the concentration of antibiotic at which bacterial growth was inhibited by 90% relative to the antibiotic-free control wells. Vancomycin, faropenem, and D-cycloserine were purchased from Sigma Aldrich (St. Louis, MO).

Additional methods can be found in the Appendix Supplementary Methods.

Expanded View for this article is available online.

Acknowledgements

We are grateful to Dr. Carl Nathan for discussions and critical reading of the manuscript. We thank Dr. Dirk Schnappinger and Dr. Kyu Rhee for helpful discussions and insightful advice. We thank Dr. Eric Rubin (Harvard School of Public Health) for the Msm RipAB KD strain, Dr. Martin Pavelka for the RipA-KO strains, and Dr. Ouathek Ouerfelli and Guangli Yang (Organic Synthesis Core Facility at Memorial Sloan Kettering Cancer Center) for the synthesis of the fluorescent D-alanine analogs. We thank Dr. Henrik Molina and Joe Fernandez of the Proteomics Resource Center at The Rockefeller University for LC-MS/MS analysis and Drs. Alison North and Kaye Thomas at the Bio-Imaging Resource Center (Rockefeller University) for invaluable help and advice. This work was supported by National Institutes of Health (NIH) R01 AI081725 and U19 AI107774. H.B. was supported by a 2-year fellowship from The Potts Memorial Foundation. MSG is supported by P30 CA008748.

Author contributions

HB, JV, and SE designed the study and analyzed the data. HB, JV, WX, HM, and NS performed experiments. MHL and HB performed the statistical analysis. MSG provided reagents. HB, JV, and SE wrote the manuscript with input from MSG and WX.

Conflict of interest

The authors declare that they have no conflict of interest.

References

- Abramovitch RB, Rohde KH, Hsu FF, Russell DG (2011) aprABC: a *Mycobacterium tuberculosis* complex-specific locus that modulates pH-driven adaptation to the macrophage phagosome. *Mol Microbiol* 80: 678–694
- Baker JJ, Johnson BK, Abramovitch RB (2014) Slow growth of *Mycobacterium tuberculosis* at acidic pH is regulated by phoPR and host-associated carbon sources. *Mol Microbiol* 94: 56–69
- Biswas T, Small J, Vandal O, Odaira T, Deng H, Ehrh S, Tsodikov OV (2010) Structural insight into serine protease Rv3671c that protects *M. tuberculosis* from oxidative and acidic stress. *Structure* 18: 1353–1363
- Böth D, Schneider G, Schnell R (2011) Peptidoglycan remodeling in *Mycobacterium tuberculosis*: comparison of structures and catalytic activities of RipA and RipB. *J Mol Biol* 413: 247–260
- Blublitz M, Polle L, Holland C, Heinz DW, Nimtz M, Schubert WD (2009) Structural basis for autoinhibition and activation of Auto, a virulence-associated peptidoglycan hydrolase of *Listeria monocytogenes*. *Mol Microbiol* 71: 1509–1522
- Chao MC, Kieser KJ, Minami S, Mavrici D, Aldridge BB, Fortune SM, Alber T, Rubin EJ (2013) Protein complexes and proteolytic activation of the cell wall hydrolase RipA regulate septal resolution in mycobacteria. *PLoS Pathog* 9: e1003197
- Choi SH, Baumler DJ, Kaspar CW (2000) Contribution of dps to acid stress tolerance and oxidative stress tolerance in *Escherichia coli* O157:H7. *Appl Environ Microbiol* 66: 3911–3916
- Davis KM, Mohammadi S, Isberg RR (2015) Community behavior and spatial regulation within a bacterial microcolony in deep tissue sites serves to protect against host attack. *Cell Host Microbe* 17: 21–31
- De Biase D, Lund PA (2015) The *Escherichia coli* acid stress response and its significance for pathogenesis. *Adv Appl Microbiol* 92: 49–88
- Flannagan RS, Cosío G, Grinstein S (2009) Antimicrobial mechanisms of phagocytes and bacterial evasion strategies. *Nat Rev Microbiol* 7: 355–366
- Foster JW (2004) *Escherichia coli* acid resistance: tales of an amateur acidophile. *Nat Rev Microbiol* 2: 898–907
- Gajiwala KS, Burley SK (2000) HDEA, a periplasmic protein that supports acid resistance in pathogenic enteric bacteria. *J Mol Biol* 295: 605–612
- Hett EC, Chao MC, Steyn AJ, Fortune SM, Deng LL, Rubin EJ (2007) A partner for the resuscitation-promoting factors of *Mycobacterium tuberculosis*. *Mol Microbiol* 66: 658–668
- Hett EC, Chao MC, Deng LL, Rubin EJ (2008) A mycobacterial enzyme essential for cell division synergizes with resuscitation-promoting factor. *PLoS Pathog* 4: e1000001
- Hett EC, Chao MC, Rubin EJ (2010) Interaction and modulation of two antagonistic cell wall enzymes of mycobacteria. *PLoS Pathog* 6: e1001020
- Kim BH, Kim S, Kim HG, Lee J, Lee IS, Park YK (2005) The formation of cyclopropane fatty acids in *Salmonella enterica* serovar Typhimurium. *Microbiology* 151: 209–218
- Krulwich TA, Sachs G, Padan E (2011) Molecular aspects of bacterial pH sensing and homeostasis. *Nat Rev Microbiol* 9: 330–343
- Kullen MJ, Klaenhammer TR (1999) Identification of the pH-inducible, proton-translocating F1F0-ATPase (atpBEFHAGDC) operon of *Lactobacillus acidophilus* by differential display: gene structure, cloning and characterization. *Mol Microbiol* 33: 1152–1161
- Kuru E, Hughes HV, Brown PJ, Hall E, Tekkam S, Cava F, de Pedro MA, Brun YV, Van Nieuwenhze MS (2012) In situ probing of newly synthesized peptidoglycan in live bacteria with fluorescent D-amino acids. *Angew Chem Int Ed* 51: 12519–12523
- Kuru E, Tekkam S, Hall E, Brun YV, Van Nieuwenhze MS (2015) Synthesis of fluorescent D-amino acids and their use for probing peptidoglycan synthesis and bacterial growth *in situ*. *Nat Protoc* 10: 33–52
- Levitte S, Adams KN, Berg RD, Cosma CL, Urdahl KB, Ramakrishnan L (2016) Mycobacterial acid tolerance enables phagolysosomal survival and establishment of tuberculous infection *in vivo*. *Cell Host Microbe* 20: 250–258
- Li YH, Hanna MN, Svensäter G, Ellen RP, Cvitkovitch DG (2001) Cell density modulates acid adaptation in *Streptococcus mutans*: implications for survival in biofilms. *J Bacteriol* 183: 6875–6884
- Lin J, Lee IS, Frey J, Slonczewski JL, Foster JW (1995) Comparative analysis of extreme acid survival in *Salmonella typhimurium*, *Shigella flexneri*, and *Escherichia coli*. *J Bacteriol* 177: 4097–4104
- MacMicking JD, Taylor GA, McKinney JD (2003) Immune control of *tuberculosis* by IFN- γ -inducible LRG-47. *Science* 302: 654–659
- Manina G, Dhar N, McKinney JD (2015) Stress and host immunity amplify *Mycobacterium tuberculosis* phenotypic heterogeneity and induce nongrowing metabolically active forms. *Cell Host Microbe* 17: 32–46
- Maroncle N, Rich C, Forestier C (2006) The role of *Klebsiella pneumoniae* urease in intestinal colonization and resistance to gastrointestinal stress. *Res Microbiol* 157: 184–193

- Martinelli DJ, Pavelka MS (2016) The RipA and RipB peptidoglycan endopeptidases are individually non-essential to *Mycobacterium smegmatis*. *J Bacteriol* 198: 1464–1475
- Martín-Galiano AJ, Ferrándiz MJ, de la Campa AG (2001) The promoter of the operon encoding the FOF1 ATPase of *Streptococcus pneumoniae* is inducible by pH. *Mol Microbiol* 41: 1327–1338
- Mujacic M, Baneyx F (2007) Chaperone Hsp31 contributes to acid resistance in stationary-phase *Escherichia coli*. *Appl Environ Microbiol* 73: 1014–1018
- Pédélec JD, Cabantous S, Tran T, Terwilliger TC, Waldo GS (2006) Engineering and characterization of a superfolder green fluorescent protein. *Nat Biotechnol* 24: 79–88
- Peters NT, Morlot C, Yang DC, Uehara T, Vernet T, Bernhardt TG (2013) Structure-function analysis of the LytM domain of EnvC, an activator of cell wall remodelling at the *Escherichia coli* division site. *Mol Microbiol* 89: 690–701
- Pham TT, Jacobs-Sera D, Pedulla ML, Hendrix RW, Hatfull GF (2007) Comparative genomic analysis of mycobacteriophage Tweety: evolutionary insights and construction of compatible site-specific integration vectors for mycobacteria. *Microbiology* 153: 2711–2723
- Ruggiero A, Marasco D, Squeglia F, Soldini S, Pedone E, Pedone C, Berisio R (2010) Structure and functional regulation of RipA, a mycobacterial enzyme essential for daughter cell separation. *Structure* 18: 1184–1190
- Schaible UE, Sturgill-Koszycki S, Schlesinger PH, Russell DG (1998) Cytokine activation leads to acidification and increases maturation of *Mycobacterium avium*-containing phagosomes in murine macrophages. *J Immunol* 160: 1290–1296
- Shabala L, Ross T (2008) Cyclopropane fatty acids improve *Escherichia coli* survival in acidified minimal media by reducing membrane permeability to H⁺ and enhanced ability to extrude H⁺. *Res Microbiol* 159: 458–461
- Singh SK, Parveen S, SaiSree L, Reddy M (2015) Regulated proteolysis of a cross-link-specific peptidoglycan hydrolase contributes to bacterial morphogenesis. *Proc Natl Acad Sci USA* 112: 10956–10961
- Small JL, O'Donoghue AJ, Boritsch EC, Tsodikov OV, Knudsen GM, Vandal O, Craik CS, Ehrt S (2013) Substrate specificity of MarP, a periplasmic protease required for resistance to acid and oxidative stress in *Mycobacterium tuberculosis*. *J Biol Chem* 288: 12489–12499
- Song H, Huff J, Janik K, Walter K, Keller C, Ehlers S, Bossmann SH, Niederweis M (2011) Expression of the ompATb operon accelerates ammonia secretion and adaptation of *Mycobacterium tuberculosis* to acidic environments. *Mol Microbiol* 80: 900–918
- Ting LM, Kim AC, Cattamanchi A, Ernst JD (1999) *Mycobacterium tuberculosis* inhibits IFN-gamma transcriptional responses without inhibiting activation of STAT1. *J Immunol* 163: 3898–3906
- Typas A, Banzhaf M, Gross CA, Vollmer W (2012) From the regulation of peptidoglycan synthesis to bacterial growth and morphology. *Nat Rev Microbiol* 10: 123–136
- Uehara T, Parzych KR, Dinh T, Bernhardt TG (2010) Daughter cell separation is controlled by cytokinetic ring-activated cell wall hydrolysis. *EMBO J* 29: 1412–1422
- Vandal OH, Pierini LM, Schnappinger D, Nathan CF, Ehrt S (2008) A membrane protein preserves intrabacterial pH in intraphagosomal *Mycobacterium tuberculosis*. *Nat Med* 14: 849–854
- Vaubourgeix J, Lin G, Dhar N, Chenouard N, Jiang X, Botella H, Lupoli T, Mariani O, Yang G, Ouerfelli O, Unser M, Schnappinger D, McKinney J, Nathan C (2015) Stressed mycobacteria use the chaperone ClpB to sequester irreversibly oxidized proteins asymmetrically within and between cells. *Cell Host Microbe* 17: 178–190
- Via LE, Fratti RA, McFalone M, Pagan-Ramos E, Deretic D, Deretic V (1998) Effects of cytokines on mycobacterial phagosome maturation. *J Cell Sci* 111(Pt 7): 897–905
- Walters SB, Dubnau E, Kolesnikova I, Laval F, Daffe M, Smith I (2006) The *Mycobacterium tuberculosis* PhoPR two-component system regulates genes essential for virulence and complex lipid biosynthesis. *Mol Microbiol* 60: 312–330
- Weiss G, Schaible UE (2015) Macrophage defense mechanisms against intracellular bacteria. *Immunol Rev* 264: 182–203
- Wen ZT, Burne RA (2004) LuxS-mediated signaling in *Streptococcus mutans* is involved in regulation of acid and oxidative stress tolerance and biofilm formation. *J Bacteriol* 186: 2682–2691
- Williams P, Cámara M (2009) Quorum sensing and environmental adaptation in *Pseudomonas aeruginosa*: a tale of regulatory networks and multifunctional signal molecules. *Curr Opin Microbiol* 12: 182–191
- Yang DC, Peters NT, Parzych KR, Uehara T, Markovski M, Bernhardt TG (2011) An ATP-binding cassette transporter-like complex governs cell-wall hydrolysis at the bacterial cytokinetic ring. *Proc Natl Acad Sci USA* 108: E1052–E1060
- Zhao N, Darby CM, Small J, Bachovchin DA, Jiang X, Burns-Huang KE, Botella H, Ehrt S, Boger DL, Anderson ED et al (2015) Target-based screen against a periplasmic serine protease that regulates intrabacterial pH homeostasis in *Mycobacterium tuberculosis*. *ACS Chem Biol* 10: 364–371